STRUCTURAL RESPONSE OF FRAMES BEFORE AND AFTER THE PLACING OF INFILL WALLS

by

DAWSON, R.V.[(i)] and WARD, M. A.[(ii)]

Summary

A 4-storey steel framed model structure is described. In order to demonstrate the stiffening effect of floors and walls, tests are reported at three phases in the construction of the model:

(1) Steel frame without floors or infill walls
(2) Steel frame with floors in place but without infill walls
(3) Steel frame with floors and infill walls in place

At each phase, static tests were carried out in which horizontal lateral load was applied at the floor levels. Results of the static tests are used to predict natural frequencies of vibration and these are compared with values found experimentally by means of sinusoidal and random vibration tests.

(i) Graduate Research Student and (ii) Associate Professor in the Civil Engineering Department of The University of Calgary.

Introduction

In the analysis of structural frames for lateral loads such as arise from earthquake or wind, the presence of non-load bearing infill walls is often neglected. In fact such walls can have a significant effect on both the static and dynamic structural response. Using structural models a research program into the effect of infill walls is being carried out at present at The University of Calgary. Preliminary work designed to demonstrate the change in response resulting from the presence of infill walls involved static and dynamic tests on a 4-storey steel model before and after infill walls were placed.

Model Structure(i)

The model described herein does not represent an existing real structure. Rather a one-sixth scale model has been constructed of a "reasonable" but rather idealized and simplified structure. The model is that of a single-bay, 4-storey steel structure with concrete floors. Figures 1 and 2 show the prototype structure and working drawings of the steel framework for the model respectively. The beam and column I-sections were milled from annealed steel and all joints were brazed using silver solder. The possibility of welding the beam column connections was investigated but in trial joints it was not possible to prevent holes being burned in the thin webs of the sections. Since the fusion temperature of silver solder is lower than the melting point of steel, this problem did not exist when the joints were brazed. Moment-rotation tests of individual joints showed that the brazed joints performed effectively even at large rotations, local failure always occuring in the beam and column sections. Rigid foundations were achieved by welding the bottom of the columns to heavy steel blocks (figure 3) which were bolted to the steel channels forming the foundation.

The floors were cast from a sand-cement mortar and contained wire mesh reinforcement. Shear connectors on the top flanges of all beams provided continuity between beams and floors.

The infill walls were ½" thick and were cast in situ using a mortar with a sand-cement ratio of 5.2 and a water-cement ratio of 1.1. The mortar had a dry density of 121 lbs./ft.^{3} and dynamic modulus testing of 12" cylinders gave a Young's Modulus of 1.95 x 10^6 p.s.i.

The formwork for the inside face of each wall consisted of a single sheet of ¼" plywood cut to fit the rectangular area enclosed by the two columns, the top beam and the concrete floor. The form for the outside face of the wall was similar except that a gap about 1" deep was left between the top of the form and the bottom flange of the beam. The two forms were spaced with their inside faces ½" apart and were bolted together in the steel frame of the model (figure 4). The mortar was gravity poured through the gap in the form and tamped with lengths of flexible wire. All eight walls in the model were cast at the same time and as the model was sitting on a shake table during casting, it was possible to lightly vibrate the whole structure. Finally the gap at the top of each wall was poured

---

(i) More detailed information on the model structure can be found in Reference 1.

and tamped, a strip of plywood being clamped on to cover the gap. (Some difficulty was encountered in obtaining good contact between the top of the wall and the lower flange of the beam. In subsequent walls, not described in this paper, this contact was improved by the use of expansive cement instead of ordinary Portland cement in the wall mortar.)

Description of Static Tests

Static lateral load tests were carried out at three phases in the model development: (1) steel frame without floors or infill walls, (2) steel frame with floors in place but without infill walls, and (3) steel frame with floors and infill walls in place.

Figure 5 shows a general view of the test set up. The model was rigidly bolted to the shake table and the table was fixed to prevent movement. The magnitude of the applied lateral load was measured using a mechanical force transducer. Dial gauges were used to measure deflection at both sides of the structure in the direction of the applied load. The test procedure was followed with the horizontal load being applied at each floor level successively and separately.

The coordinate system of figure 6 is used in future discussion of structural flexibility.

Static Test Results

Phase (1) Steel frame without floors or infill walls.

The load-deflection relationships obtained when the horizontal load was applied at coordinate 3 are shown in figure 7. These curves are approximately linear. Similar curves were obtained from tests with loads applied at the other floor levels. The following flexibility matrix was obtained for the complete three-dimensional model by measuring the slopes of the static load deflection curves:

$$[f]_{e1} = \begin{vmatrix} 0.00166 & 0.00121 & 0.00088 & 0.00034 \\ 0.00123 & 0.00104 & 0.00086 & 0.00034 \\ 0.00078 & 0.00076 & 0.00076 & 0.00034 \\ 0.00035 & 0.00034 & 0.00034 & 0.00024 \end{vmatrix} \text{ ins./lb.}$$

If the model is analysed as a two-dimensional linear elastic ($E = 30 \times 10^6$ p.s.i.) plane frame with axial deformations in the columns being taken into account, small deformation theory of structures leads to the following flexibility matrix:

$$[f]_1 = \begin{vmatrix} 0.00141 & 0.00106 & 0.00065 & 0.00026 \\ 0.00106 & 0.00098 & 0.00064 & 0.00026 \\ 0.00065 & 0.00064 & 0.00057 & 0.00025 \\ 0.00026 & 0.00026 & 0.00025 & 0.00020 \end{vmatrix} \text{ ins./lb.}$$

As a consequence of Maxwell's Reciprocal Theorem, $[f]_1$ is symmetrical. The lack of symmetry observed in $[f]_{e1}$ is due to a combination of nonlinearities in the structural behaviour and experimental error. Reasonable symmetry exists in $[f]_{e1}$ except in the third column and third row where the corresponding elements differ by as much as 13 per cent. Since the elements of each column of $[f]_{e1}$ were derived from a single loading condition whereas

the elements of each row were derived from four different loading conditions, it is more likely that the elements of a single column of the matrix will be in error by a constant factor than the elements of a single row. If the third column of $[f]_{e1}$ is multiplied by 0.89, then $[f]_{e1}$ becomes:

$$\begin{vmatrix} 0.00166 & 0.00121 & 0.00078 & 0.00034 \\ 0.00123 & 0.00104 & 0.00076 & 0.00034 \\ 0.00078 & 0.00076 & 0.00068 & 0.00034 \\ 0.00035 & 0.00034 & 0.00030 & 0.00024 \end{vmatrix} \text{ ins./lb.} \quad (A)$$

Further justification for the above modification to $[f]_{e1}$ comes from consideration of the diagonal elements of $[f]_{e1}$ and $[f]_2$.

If E is a vector such at $(E_i) = \frac{(fii)_{e1}}{(fii)_1}$, then

$$\{E\} = \begin{vmatrix} 1.22 \\ 1.11 \\ 1.36 \\ 1.20 \end{vmatrix}$$

$(E_3) = 1.36$ is considerably greater than the other elements, but if it is multiplied by 0.89 it becomes 1.21. This correlates better with the other elements of {E}.

The final modified experimental flexibility matrix is made symmetrical by averaging the appropriate elements of matrix (A):

$$[f]_{me1} = \begin{vmatrix} 0.00166 & 0.00122 & 0.00078 & 0.00035 \\ 0.00122 & 0.00104 & 0.00076 & 0.00034 \\ 0.00078 & 0.00076 & 0.00068 & 0.00032 \\ 0.00035 & 0.00034 & 0.00032 & 0.00025 \end{vmatrix} \text{ ins./lb.}$$

It is interesting to compare the experimentally derived flexibility matric $[f]_{me1}$ with the theoretical matrix $[f]_1$.

The model is seen to be more flexible than was theoretically predicted from knowledge of the frame dimensions and section sizes. A discrepancy as high as 26 per cent occurs in the elements of the first row and fourth columns of the flexibility matrices. The largest error in the more important diagonal terms is 17 per cent. Possibly some of the added flexibility was contributed by local deformations in the brazed connections.

Phase (2) Steel frame with floors in place but without infill walls.

Static tests similar to those carried out at Phase (1) were performed after floors had been cast in the model and masses added to the floors to simulate dead load effects. Measurement of the slopes of the load deflection curves (figure 7) led to the following flexibility matrix:

$$[f]_{e2} \begin{vmatrix} 0.00173 & 0.00113 & 0.000758 & 0.00019 \\ 0.00142 & 0.00104 & 0.000739 & 0.00018 \\ 0.00087 & 0.00069 & 0.000578 & 0.00018 \\ 0.00039 & 0.00029 & 0.000234 & 0.00014 \end{vmatrix} \text{ ins./lbs.}$$

Critical examination of this flexibility matrix in a similar manner to that described in Phase (1) led to the modified symmetrical experimental

flexibility matrix:

$$[f]_{me2} = \begin{vmatrix} 0.0015 & 0.0011 & 0.0007 & 0.0002 \\ 0.0011 & 0.0010 & 0.0007 & 0.0002 \\ 0.0007 & 0.0007 & 0.0006 & 0.0002 \\ 0.0002 & 0.0002 & 0.0002 & 0.0002 \end{vmatrix} \text{ ins./lb.}$$

Comparing this matrix with $[f]_{me1}$ it can be seen that, as expected, the addition of floors to the model has increased its stiffness by about 10 per cent. The beams acting in conjunction with the floors were stiff compared to the columns and displacements at the floor levels therefore resulted mainly from bending deformations in the columns. This is typical of a "shear" type structure where the relative displacement between two adjacent floors is dependent only on the shear between the two floors.

Phase (3) Steel frame with floors and infill walls.

Static load-deflection relationships at Phase 3 are shown in figure 8 for all four loading cases. The behaviour of the structure is similar to that of a hardening spring. Each load-deflection curve can be approximated by two linear portions with a connecting curved portion.

It is interesting to compare the initial slopes of these curves with those values obtained before the walls were present. Matrix $[f]_{e3}$ is an array of the initial slopes of the curves of figure 8.

$$[f]_{e3} = \begin{vmatrix} 0.00062 & 0.00042 & 0.00017 & 0.00010 \\ 0.00050 & 0.00040 & 0.00018 & 0.00010 \\ 0.00034 & 0.00029 & 0.00018 & 0.00009 \\ 0.00015 & 0.00014 & 0.00008 & 0.00008 \end{vmatrix} \text{ ins./lb.}$$

Lack of symmetry in the elements of this matrix is more evident than in $[f]_{e2}$ (before the walls were placed). Comparison of $[f]_{e3}$ and $[f]_{me2}$ indicates that even the initial linear region of loading, and walls did have considerable stiffening effect and the model flexibility was reduced by more than 50 per cent as a result of the inclusion of the infill walls. However in this region the bending stiffness of the frame still presents an important contribution to the total stiffness.

The curved portion of the load-deflection curves represents the transition to a stage where the walls are fully active structurally. By limiting bending deformations in the columns, the walls cause the mode of structural action to change from bending frame action to one where the walls behave in a similar manner to diagonal compression struts. In doing so the walls cause a major increase in the structural stiffness. Observation of, say, the fourth floor deflections in figure 8 indicates that the structural behaviour is now totally dissimilar to a simple "shear" structure. The deflection is a function not only of the magnitude of the applied load but also is significantly dependent on the location of the load.

A symmetrical flexibility matrix was obtained by averaging the appropriate elements of $[f]_{e3}$.

$$[f]_{me3} = \begin{vmatrix} 0.00062 & 0.00046 & 0.00025 & 0.00013 \\ 0.00046 & 0.00040 & 0.00025 & 0.00012 \\ 0.00025 & 0.00025 & 0.00018 & 0.00009 \\ 0.00013 & 0.00012 & 0.00009 & 0.00008 \end{vmatrix} \text{ ins./lb.}$$

Natural Frequencies

If [M] is the mass matrix of a structure, {D} the displacement rector and [f] the flexibility matrix for the same coordinate system as {D}, then the equation for free vibration of the structure is:

$$[f][M]\{D\} = \frac{1}{\omega^2}\{D\} \qquad (1)$$

where ω is the radial frequency of free vibration.

For the present model the mass was assumed to be lumped equally at all floor levels. The mass matrices at the various phases were:

$$[M]_1 = \begin{vmatrix} 11.85 & 0. & 0. & 0. \\ 0. & 11.85 & 0. & 0. \\ 0. & 0. & 11.85 & 0. \\ 0. & 0. & 0. & 11.85 \end{vmatrix} \text{ lbs.}$$

$$[M]_2 = \begin{vmatrix} 516. & 0. & 0. & 0. \\ 0. & 516. & 0. & 0. \\ 0. & 0. & 516. & 0. \\ 0. & 0. & 0. & 516. \end{vmatrix} \text{ lbs.}$$

$$[M]_3 = \begin{vmatrix} 529. & 0. & 0. & 0. \\ 0. & 529. & 0. & 0. \\ 0. & 0. & 529. & 0. \\ 0. & 0. & 0. & 529. \end{vmatrix} \text{ lbs.}$$

The eigenvalue equation (1) was solved for the model at Phase (1) using $[M]_1$ and $[f]_{me1}$, at Phase (2) using $[M]_2$ and $[f]_{me2}$ and at Phase (3) using $[M]_3$ and $[f]_{me3}$. The theoretical natural frequencies obtained are shown in Table I.

It must be pointed out that because of the lack of symmetry which existed in $[f]_{e3}$ and the nonlinearities involved when the walls are present in the model, the analysis at Phase (3) is very approximate.

Dynamic Tests

The shake table [2,3] used to generate sinusoidal and random base motion in the model is driven by an electrohydraulic closed-look system. Figure 9 shows a general view of the model (with walls in place)on the shake table.

Sinusoidal Tests

Sinusoidal vibration tests were carried out in order to investigate the natural frequencies of the model at Phases (1) and (2) of construction. The output of an accelerometer located at the top floor of the model was observed on an oscilloscope. Since peak accelerations occur at resonance, it was possible to sweep slowly through various frequencies of sinusoidal base motion and locate resonances in the structure. Table I shows the natural frequencies identified in this manner. At Phase (1) of construction it was possible to identify two natural frequencies within the operating range of the shaker system. All four natural frequencies were identified at Phase (2). Good correlation was found between predicted and measured

natural frequencies, the error being greater in the higher than in the lower modes. Predictions at Phase (2) were better than at Phase (1). This was to be expected since the lumped mass model was more realistic at Phase (2) when there were large masses located at the floor levels. At Phase (1) the columns between floor levels represented a more significant proportion of the total mass of the model. It was possible that some deterioration of the walls and change in their structural behaviour could occur during dynamic testing. Thus, at Phase (3) sinusoidal tests were not performed, the initial dynamic test being a random vibration test.

Random Vibration Tests

At Phases (2) and (3) of construction of the model, the shake table was subjected to white noise acceleration. Strains at several locations in the model were recorded. For present purposes, the output of a strain gauge located as shown schematically in figure 6 shall be considered. A Fourier Analyzer System (Hewlett-Packard Model 5450A) was used to automatically obtain plots of power spectral density vs. frequency for the strain signal.

Figure 10(a) shows the power spectrum obtained at Phase (2) of construction of the model. The resonances occurring at frequencies corresponding to the first three natural frequencies are obvious. The vertical scale was multiplied by a factor of 100 (figure 10(b)) and it was then possible to identify the fourth mode. It can be seen that the major response was derived from the first mode and that the participation of each mode to the total response decreased at the mode number increased. The natural frequencies derived from figure 10 are recorded in Table I. The values obtained from random tests are seen to be in all cases slightly less than those obtained from the sinusoidal tests. The difference is very small and is probably due to "loosening" of the structure during the sinusoidal tests causing a slight decrease in stiffness of the structure for the subsequent random tests.

Figure 11 shows the power spectrum obtained at Phase (3), after the walls had been placed. A limitation of this spectral analysis is that strictly speaking it should be applied to a linear model. However it is interesting to observe that significant responses occur in the range $0 \rightarrow 5$ c.p.s. and there is an obvious resonance at 3.4 c.p.s. This appears to be the fundamental mode, which has been raised from 2.4 c.p.s. due to the stiffening effect of the walls. The theoretical value for the fundamental frequency at Phase (3) was 4.0 c.p.s., which compares favourably with the measured resonance at 3.4 c.p.s. The approximate nature of the theoretical analysis has already been pointed out. It is only considered in order to illustrate that the increase in the fundamental frequency when the walls are placed is of the same order as might be expected from considerations of the increased stiffness of the structure in the initial linear region of the static response curves.

The presence of the walls appears to have had the additional effect of damping out participation of the higher modes.

Conclusions

A 4-storey steel framed model structure has been described. Static lateral load tests carried out at various stages in the construction of the model have demonstrated the additional stiffness provided by floors and infill walls.

Sinusoidal and random vibration tests carried out before the walls were present proved that the static test results could be used to obtain good prediction of natural frequencies, particularly in the lower modes. Random vibration testing of the model with infill walls in place showed that response was primarily in a fundamental mode at a frequency higher than the fundamental frequency before the walls were present.

ACKNOWLEDGEMENT

This work is supported by a contract held by The University of Calgary with Canadian Emergency Measures Organization, Department of National Defence, Ottawa.

BIBLIOGRAPHY

1. Ward, M.A., "Response of Steel Frame Buildings to Dynamic Loads", Canadian Emergency Measures Organization, File No.202-2-15,April 1970.

2. Ward, M.A. and Dawson,R.V., "A High Force Shake Table for Earthquake Simulation", RILEM International Symposium on Methodology and Technique of Testing Structures, Bucharest, September 1969.

3. Dawson, R.V. and Ward, M.A., "The Design and Performance of a High-Force Shake Table for Earthquake Simulation", presented at Soc. for Exper. Stress Analysis Fall Meeting, Houston, October 1969.

TABLE I

THEORETICAL AND EXPERIMENTAL NATURAL FREQUENCIES

Mode of Vibration	NATURAL FREQUENCIES (C.P.S.)						
	Phase (1)		Phase (2)			Phase (3)	
	Sinusoidal Test	Predicted(i)	Sinusoidal Test	Random Vibr. Test	Predicted(i)	Random Vibr. Test	Predicted(i)
1	16.6	16.0	2.6	2.4	2.6	3.4	4.0
2	47.7	45.6	8.1	8.0	8.2	-	14.1
3	--	102.4	14.2	14.0	12.4	-	23.4
4	--	197.6	19.8	19.4	23.7	-	90.4

(i) Predicted values are based on flexibility matrices derived from static tests.

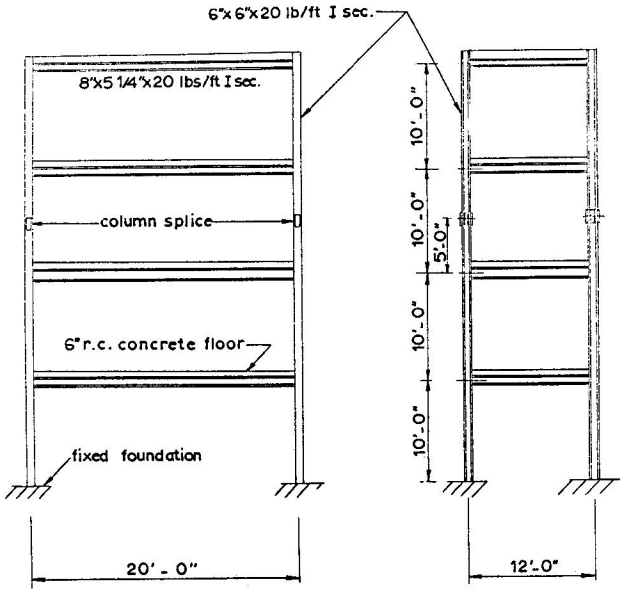

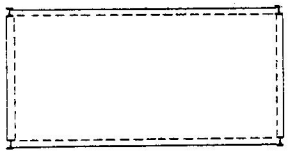

N O T E : All joints welded.

T E S T S T R U C T U R E
(model is 1/6 scale)

Figure 1 Prototype Structure

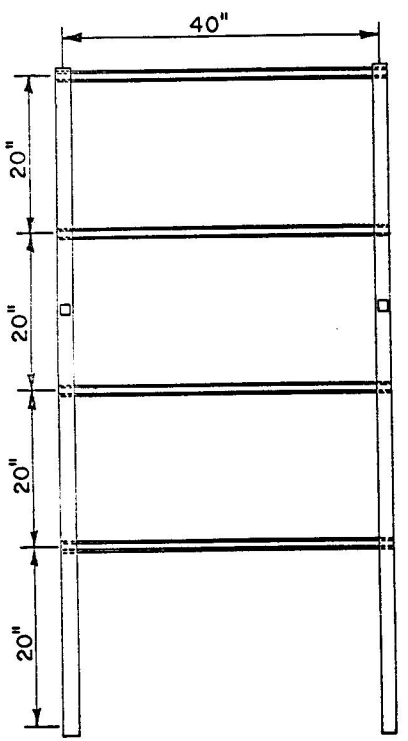

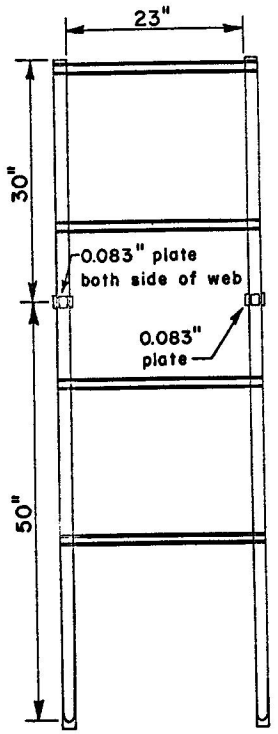

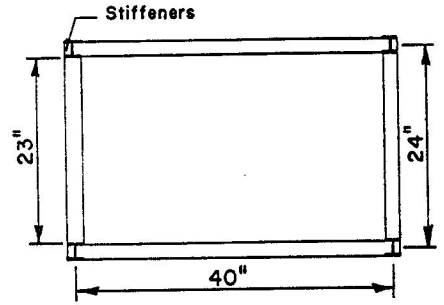

Note: All stiffeners at beam column connections have the same thickness as the beam flange.

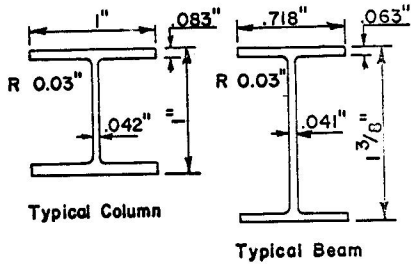

Figure 2 Steel Framework for Model

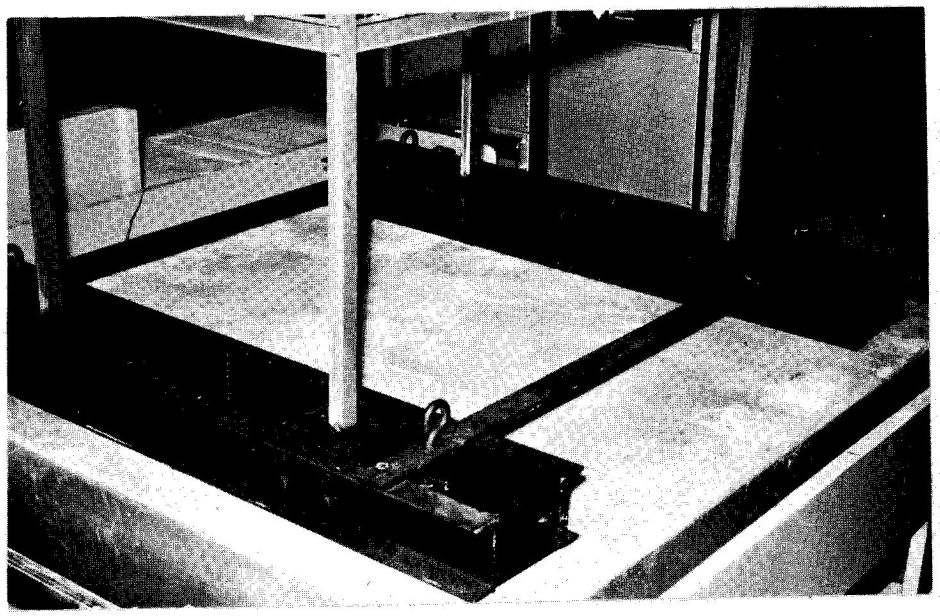

Figure 3 Rigid Foundation

Figure 4 Formwork for Infill Wall

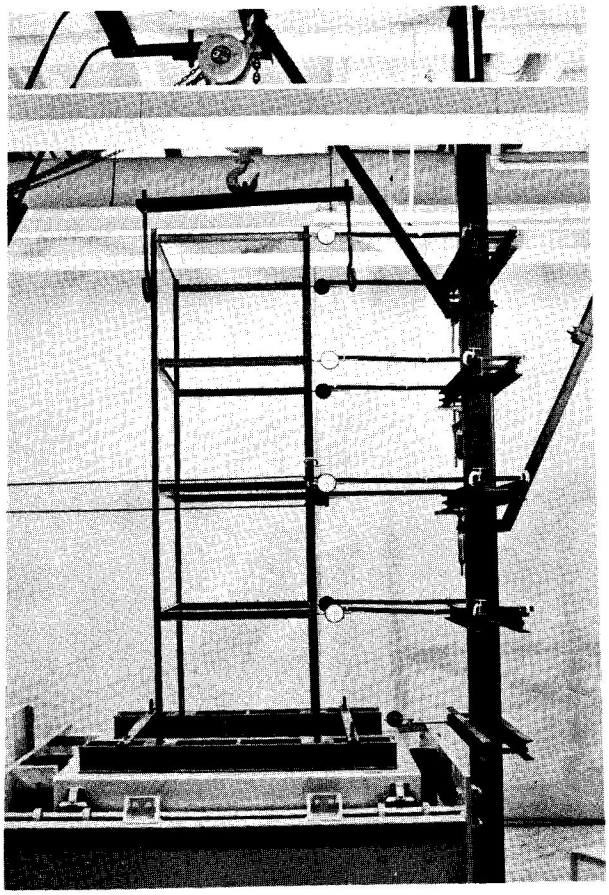

Figure 5 Static Flexibility Test

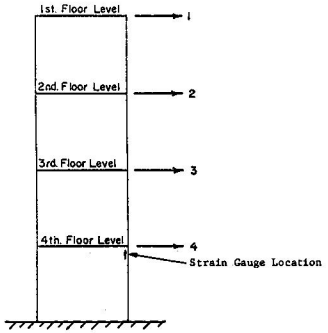

Figure 6 Coordinate System

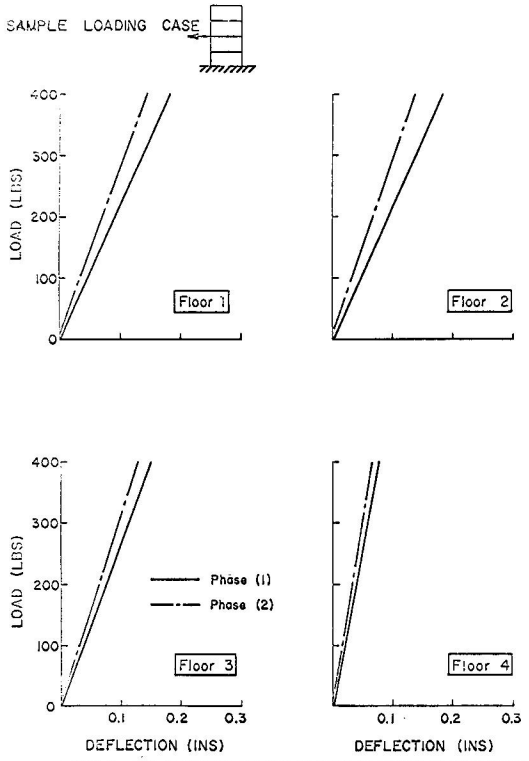

Figure 7 Load-Deflection Relations at Phase (1) and (2) of Construction Load Applied at Floor 3

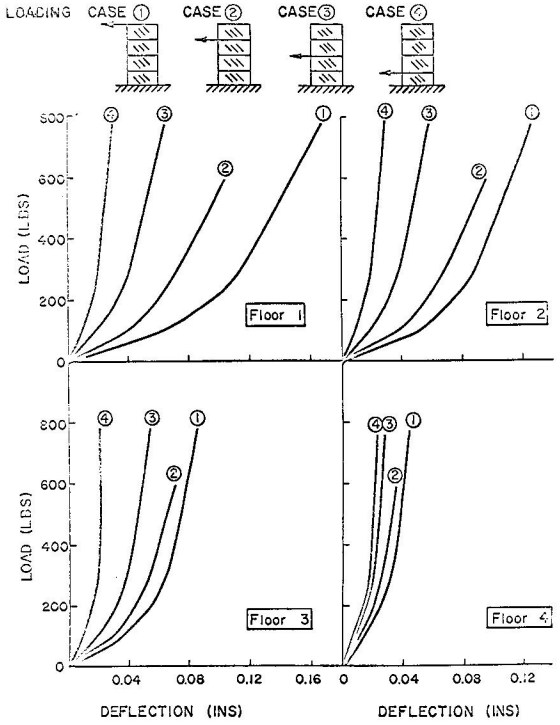

Figure 8 Load-Deflection Relations at Phase (3) of Construction

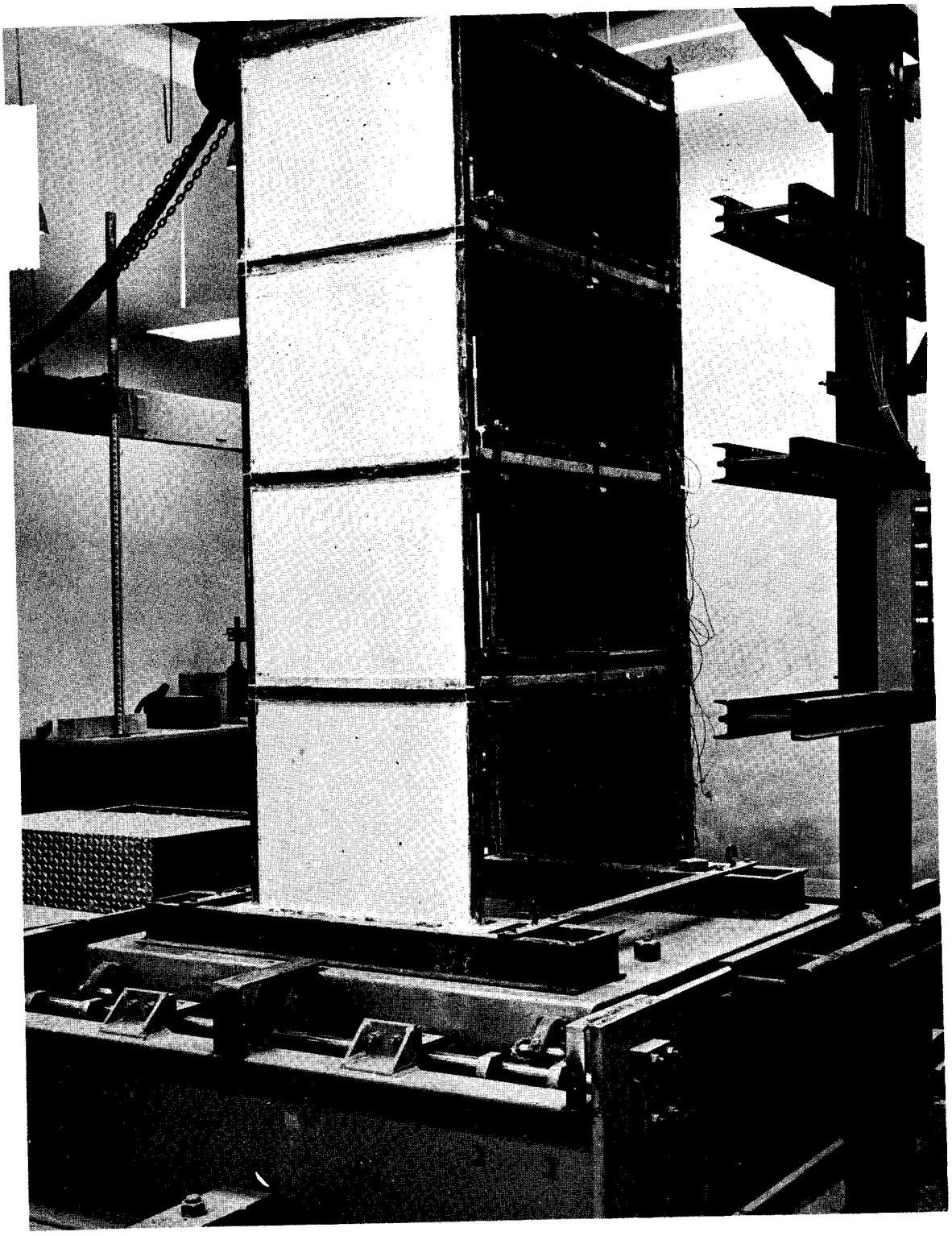

Figure 9 General View of Model on Shake Table

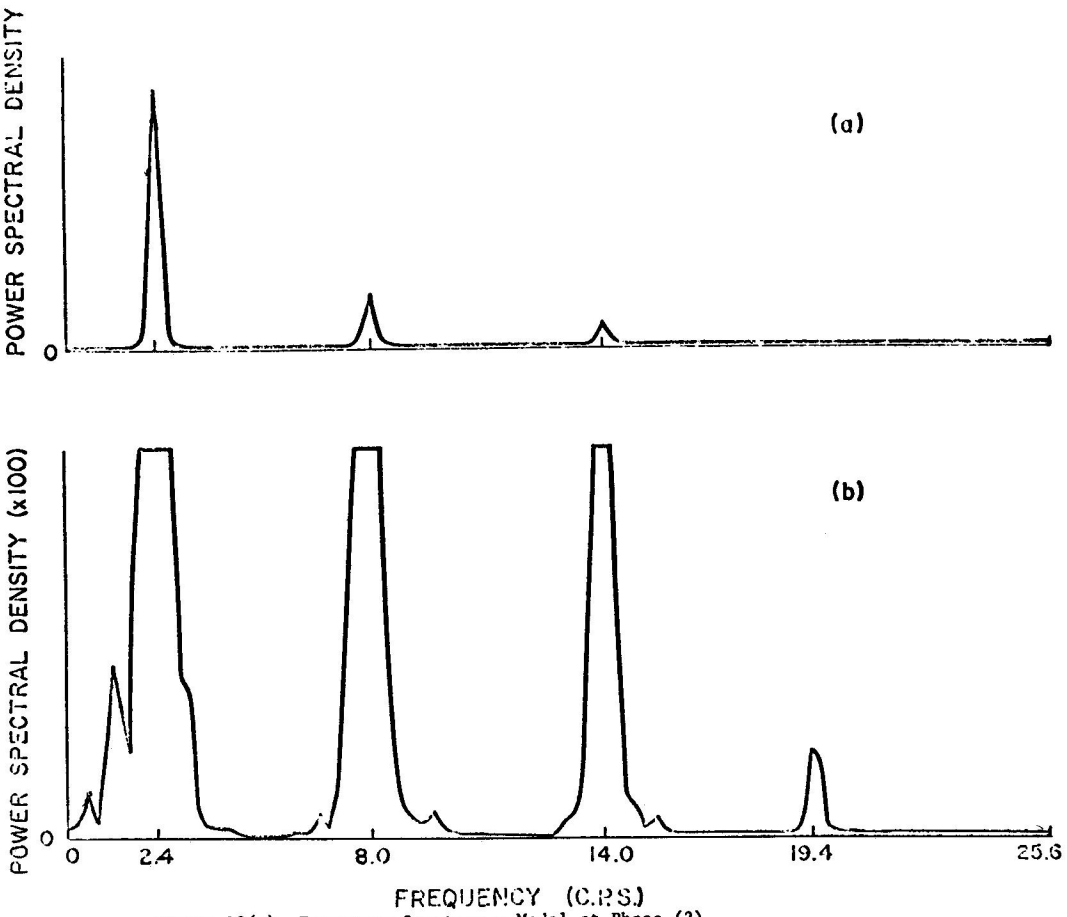

Figure 10(a) Frequency Spectrum - Model at Phase (2)
(b) Frequency Spectrum - Model at Phase (2) (Vertical scale x 100)

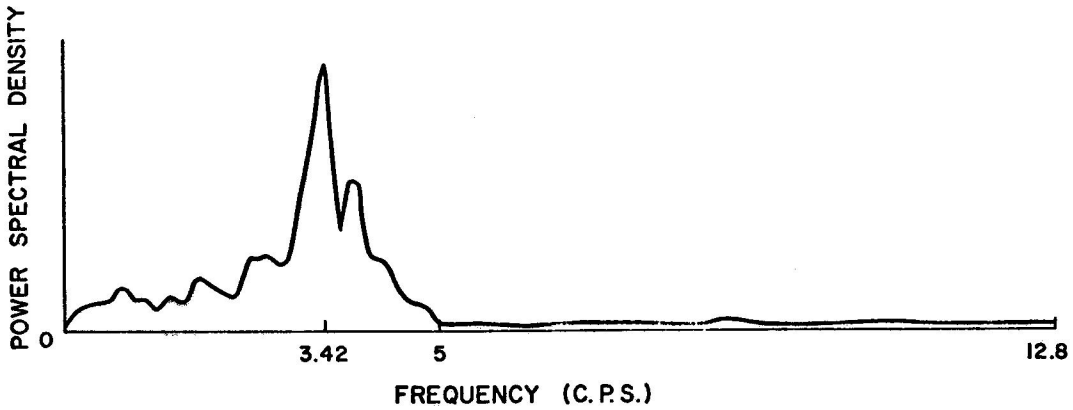

Figure 11 Frequency Spectrum - Model at Phase (3)

DISCUSSION OF PAPER NO. 20

STRUCTURAL RESPONSE OF FRAMES CONTAINING INFILL WALLS

by

R.V. Dawson and M.A. Ward

Discussion by: Y.P. Gupta

The authors have carried out the load-deformation tests for the frame in only one direction of loading while the dynamic loading is in both directions. The properties and hysteresis may be quite different. A reversed loading test would give more realistic characteristics.

Reply by: R.V. Dawson

The model structure at Phases (1) and (2) of construction behaved elastically so no hysteresis effects would be expected.

At Phase (3) of construction static cyclic load deformation tests would provide additional information about the damping characteristics. However, in the approximate analysis for natural frequencies damping has been neglected and the slopes provided by the initial load tests would still be valid.

Question by: A.A. Mufti

Would you describe the characteristics of a link element between rectangular elements representing wall and beam elements? How would you determine these characteristics?

Reply by: R.V. Dawson

The present paper is intended only to provide experimental demonstration of the effects of infill walls. I have however mentioned that we are carrying out a finite element analysis, so shall briefly describe the technique being used.

The walls are divided into a mesh of rectangular elements (eg. A B C D) with two translational degrees of freedom at each node.

The beams and columns are subdivided into frame elements (eg. E F and E G) with two translational and one rotational degree of freedom at each node.

Vertical link elements (eg BF) connect peripheral wall nodes to the beams and horizontal link elements (eg GC) connect peripheral wall nodes to the columns.

The wall is shown in Figure (A) to be separated from the frame. In fact the coordinates of wall nodes and corresponding frame nodes are made identical (eg A = E, G = C, F = B) and the link elements are considered to be pin jointed struts of zero length, with element stiffness matrix of the form:

$$[\,K\,] = \begin{bmatrix} k & -k \\ -k & k \end{bmatrix}$$

By using a large value for k (theoretically infinite) deflections in the frame nodes and corresponding wall nodes can be made to coincide. The limitation on the maximum value of k is that the equilibrium equations must be sufficiently well-conditioned to solve. When load is applied to the structure some link elements will act in tension and some in compression. No tension bond is considered to be present between frame and wall so all tension links are removed allowing separation to take place between frame and wall at these nodes. The structural stiffness matrix is reassembled and load reapplied. An iteration process ensues until only compression links remain to connect the wall to the frame.

The introduction of the link element concept provides a useful device for analysing interaction problem of frames with infill walls.

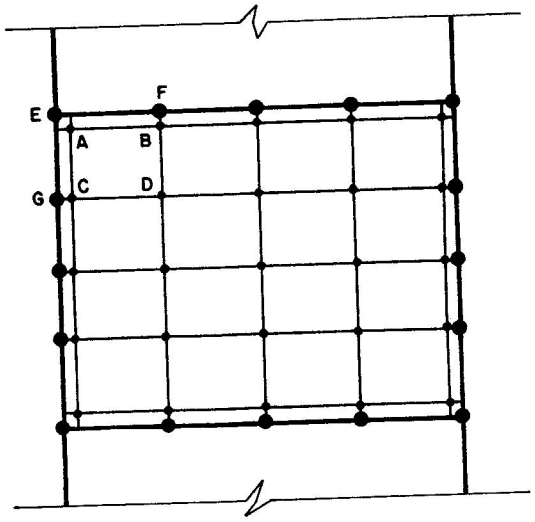

Figure(A): Typical Finite Element Mesh